ACKNOWLEDGMENT

This work was supported by Grant-in-Aid for Science Research from the Japanese Ministry of Education, Culture, Sports, Science & Technology (B-1539044) and Grant-in-Aid for New Energy and Industrial Technology Development Organization (03A04002a).

REFERENCES

1. Altman GH, Horan RL, Martin I, et al. Cell differentiation by mechanical stress. *FASEB J.* 2002;16:270-272.
2. Amiel D, Nagineni CN, Choi SH, Lee J. Intrinsic properties of ACL and MCL cells and their responses to growth factors. *Med Sci Sports Exerc.* 1995;27:844-851.
3. Anderson K, Seneviratne AM, Izawa K, Atkinson BL, Potter HG, Rodeo SA. Augmentation of tendon healing in an intraarticular bone tunnel with use of a bone growth factor. *Am J Sports Med.* 2001;29:689-698.
4. Awad HA, Butler DL, Boivin GP, et al. Autologous mesenchymal stem cell–mediated repair of tendon. *Tissue Eng.* 1999;5:267-277.
5. Bellincampi LD, Closkey RF, Prasad R, Zawadsky JP, Dunn MG. Viability of fibroblast-seeded ligament analogs after autogenous implantation. *J Orthop Res.* 1998;16:414-420.
6. Berenson MC, Blevins FT, Plaas AH, Vogel KG. Proteoglycans of human rotator cuff tendons. *J Orthop Res.* 1996;14:518-525.
7. Cao Y, Vacanti JP, Ma X, et al. Generation of neo-tendon using synthetic polymers seeded with tenocytes. *Transplant Proc.* 1994;26:3390-3392.
8. Dejardin LM, Arnoczky SP, Ewers BJ, Haut RC, Clarke RB. Tissue-engineered rotator cuff tendon using porcine small intestine submucosa. *Am J Sports Med.* 2001;29:175-184.
9. Dunn MG, Liesch JB, Tiku ML, Zawadsky JP. Development of fibroblast-seeded ligament analogs for ACL reconstruction. *J Biomed Mater Res.* 1995;29:1363-1371.
10. Frank C, Woo SL, Amiel D, Harwood F, Gomez M, Akeson W. Medial collateral ligament healing: a multidisciplinary assessment in rabbits. *Am J Sports Med.* 1983;11:379-389.
11. Funakoshi T, Majima T, Iwasaki N, et al. Novel chitosan based hyaluronan hybrid polymer fibers for a scaffold in ligament tissue engineering. *ORS Trans.* 2003;117.
12. Gentleman E, Lay AN, Dickerson DA, Nauman EA, Livesay GA, Dee KC. Mechanical characterization of collagen fibers and scaffolds for tissue engineering. *Biomaterials.* 2003;24:3805-3813.
13. Gerber C. Latissimus dorsi transfer for the treatment of irreparable tears of the rotator cuff. *Clin Orthop.* 1992;275:152-160.
14. Hu M, Sabelman EE, Lai S, et al. Polypeptide resurfacing method improves fibroblast's adhesion to hyaluronan strands. *J Biomed Mater Res.* 1999;47:79-84.
15. Koh JL, Szomor Z, Murrell GA, Warren RF. Supplementation of rotator cuff repair with a bioresorbable scaffold. *Am J Sports Med.* 2002;30:410-413.
16. Kumagai J, Sarkar K, Uhthoff HK, Okawara Y, Ooshima A. Immunohistochemical distribution of type I, II and III collagens in the rabbit supraspinatus tendon insertion. *J Anat.* 1994;185:279-284.
17. Langer R, Vacanti JP. Tissue engineering. *Science.* 1993;260:920-926.
18. Laurent TC, Fraser JR. Hyaluronan. *FASEB J.* 1992;6:2397-2404.
19. Madihally SV, Matthew HW. Porous chitosan scaffolds for tissue engineering. *Biomaterials.* 1999;20:1133-1142.
20. Majima T, Yasuda K, Yamamoto N, Kaneda K, Hayashi K. Deterioration of mechanical properties of the autograft in controlled stress–shielded augmentation procedures: an experimental study with rabbit patellar tendon. *Am J Sports Med.* 1994;22:821-829.
21. Mierisch CM, Wilson HA, Turner MA, et al. Chondrocyte transplantation into articular cartilage defects with use of calcium alginate: the fate of the cells. *J Bone Joint Surg Am.* 2003;85:1757-1767.
22. Nagineni CN, Amiel D, Green MH, Berchuck M, Akeson WH. Characterization of the intrinsic properties of the anterior cruciate and medial collateral ligament cells: an in vitro cell culture study. *J Orthop Res.* 1992;10:465-475.
23. Ostrander RV, Goomer RS, Tontz WL, et al. Donor cell fate in tissue engineering for articular cartilage repair. *Clin Orthop.* 2001;389:228-237.
24. Ouyang HW, Goh JC, Lee EH. Use of bone marrow stromal cells for tendon graft-to-bone healing: histological and immunohistochemical studies in a rabbit model. *Am J Sports Med.* 2004;32:321-327.
25. Ozaki J, Fujimoto S, Masuhara K, Tamai S, Yoshimoto S. Reconstruction of chronic massive rotator cuff tears with synthetic materials. *Clin Orthop.* 1986;202:173-183.
26. Riemersa DJ, Schamhardt HC. The cryo-jaw, a clamp designed for in vitro rheology studies of horse digital flexor tendons. *J Biomech.* 1982;15:612-620.
27. Riley GP, Harrall RL, Constant CR, Chard MD, Cawston TE, Hazleman BL. Glycosaminoglycans of human rotator cuff tendons: changes with age and in chronic rotator cuff tendonitis. *Ann Rheum Dis.* 1994;53:367-376.
28. Underhill C. CD44: the hyaluronan receptor. *J Cell Sci.* 1992;103:293-298.
29. Yamane S, Iwasaki N, Majima T, et al. Feasibility of chitosan-based hyaluronic acid hybrid biomaterial for a novel scaffold in cartilage tissue engineering. *Biomaterials.* 2005;26:611-619.
30. Young RG, Butler DL, Weber W, Caplan AI, Gordon SL, Fink DJ. Use of mesenchymal stem cells in a collagen matrix for Achilles tendon repair. *J Orthop Res.* 1998;16:406-413.
31. Zimmerman E, Geiger B, Addadi L. Initial stages of cell-matrix adhesion can be mediated and modulated by cell-surface hyaluronan. *Biophys J.* 2002;82:1848-1857.

Novel chitosan-based hyaluronan hybrid polymer fibers as a scaffold in ligament tissue engineering

Tadanao Funakoshi,[1,2] Tokifumi Majima,[1,2] Norimasa Iwasaki,[1,2] Shintaro Yamane,[1,2] Tatsuya Masuko,[1,2] Akio Minami,[1,2] Kazuo Harada,[3] Hiroshi Tamura,[5] Seiichi Tokura,[5] Shin-Ichiro Nishimura[2,4]

[1]*Department of Orthopaedic Surgery, Hokkaido University, Graduate School of Medicine, Sapporo, Japan*
[2]*Frontier Research Center for Post-genomic Science and Technology, Hokkaido University, Sapporo, Japan*
[3]*Chemical Biology Institute, Inc., Sapporo, Japan*
[4] *Laboratory of Bio-macromolecular Chemistry, Hokkaido University, Graduate School of Science, Sapporo, Japan*
[5]*Faculty of Engineering and HRC, Kansai University, Osaka, Japan*

Received 9 March 2003; revised 16 August 2004; accepted 20 October 2004
Published online 12 July 2005 in Wiley InterScience (www.interscience.wiley.com). DOI: 10.1002/jbm.a.30237

Abstract: To clarify the feasibility of using novel chitosan-based hyaluronan hybrid polymer fibers as a scaffold in ligament tissue engineering, their mechanical properties and ability to promote cellular adhesion, proliferation, and extracellular matrix production were studied *in vitro*. Chitosan fibers and chitosan-based 0.05% and 0.1% hyaluronan hybrid fibers were developed by the wet spinning method. Hyaluronan coating significantly increased mechanical properties, compared to the chitosan fibers. Rabbit fibroblasts adhesion onto hybrid fibers was significantly greater than for the control and chitosan fibers. For analysis of cell proliferation and extracellular matrix production, a three-dimensional scaffold was created by simply piling up each fiber. At 1 day after cultivation, the DNA content in the hybrid scaffolds was higher than that in the chitosan scaffold. Scanning electron microscopy showed that the fibroblasts had produced collagen fibers after 14 days of culture. Immunostaining for type I collagen was clearly predominant in the hybrid scaffolds, and the mRNA level of type I collagen in the hybrid scaffolds were significantly greater than that in the chitosan scaffold. The present study revealed that hyaluronan hybridization with chitosan fibers enhanced fiber mechanical properties and *in vitro* biological effects on the cultured fibroblasts. © 2005 Wiley Periodicals, Inc. J Biomed Mater Res 74A: 338–346, 2005

Key words: chitosan; hyaluronan; tissue engineering; ligament; scaffold

INTRODUCTION

Severe ligament injuries are frequently treated using autograft reconstruction; however, because of donor site morbidity, this surgical procedure is not ideal. To overcome this drawback, the application of tissue engineering techniques in which isolated fibroblasts are cultured on scaffold material should be considered. Several tissue-engineering studies have demonstrated successful ligament and tendon tissue regeneration using a variety of scaffold materials, including both naturally occurring and synthetic materials.[1–8] However, little attention has been given to whether or not these scaffold materials can biologically and mechanically support transplanted fibroblasts and regenerated ligament in the living body. Therefore, we may say that there are no ideal materials for ligament tissue engineering.

Tissue engineering is an emerging scientific approach that attempts to develop biological substitutes made from isolated cells and three-dimensional (3D) polymeric scaffolds.[9] The principal role of 3D scaffolds in musculoskeletal tissue engineering, including ligament tissue engineering, is to provide a temporary template with the biomechanical characteristics of the native extracellular matrix (ECM) during the process of *in vivo* tissue regeneration. Additionally, in living organisms, the authentic substrate for most cells is the ECM. The ECM adheres to cells via integrins, which are membrane-spanning heterodimeric receptors. Through cell–ECM adhesion, the ECM transduces physiological signals regulating cell growth, cell proliferation, cell differentiation, and matrix remodeling to the cells.[10] The ECM not only binds embedded cells

Correspondence to: T. Funakoshi, Department of Orthopaedic Surgery, Hokkaido University School of Medicine, North 15 West 7, Kita–Ku, Sapporo 060–8638, Japan; e-mail: t-funa@med.hokudai.ac.jp

Contract grant sponsor: Japan Ministry of Education, Culture, Sports, Science, & Technology; contract grant numbers: B–1539044, 03A04002a

together but also affects their survival, development, shape, polarity, and behavior. Therefore, the ECM plays an important role in living tissue development and regeneration. For these reasons, we believe that the ideal scaffold material should be one that closely mimics the natural environment in the ECM.

Some materials, including collagen gels, collagen sponges, and collagen constructs, have been used as scaffolds in ligament tissue engineering[2–5] but these materials do not structurally mimic ligament-specific ECM. Consequently, in the living body, they do not provide sufficient mechanical support for the regenerated ligament, or transduce mechanophysiological signals that significantly enhance ligament regeneration and remodeling processes, to the embedded cells. In addition, given the importance of glycosaminoglycans (GAGs) in stimulating various *in vitro* tissue regenerative processes, the use of GAGs or GAG-like materials as components of a scaffold should be a reasonable approach for ligament tissue engineering. Hyaluronan (HA), which is the main component of the GAGs, has been shown to improve healing in a variety of tissues through the effects on delivery of growth factors, cellular adhesion, and proliferation, and anti-inflammatory reactions.[11–14] These biological effects of HA would also play a crucial role in enhancing ligament tissue regeneration. On the other hand, chitosan has been employed as an excellent biocompatible material in wound healing and tissue repair,[15] and because it is regarded as a cationic polysaccharide showing excellent cell adhesive properties, hybrid materials composed of chitosan combined with HA might provide a novel class of polyion complex effective as for ligament-specific scaffold materials.

Tamura and colleagues established a new methodology for preparation of chitosan-coated GAG-mimicking filaments.[16] They also showed enhancement of mechanical strength of the GAG-mimicking filaments by coating chitosan through ionic interaction. To mimic the natural environment of ligament ECM, based on their methodology, we have developed a novel hybrid-polymer fiber — a chitosan-based HA hybrid polymer fiber — as a fundamental material for ligament-specific scaffolds.

In the current study, we hypothesized that HA could enhance the mechanical strength of the hybrid polymer fiber and impart superior biological effects on the fibroblasts in a 3D culture system. To test our hypothesis, we measured the mechanical strength of the chitosan-based HA hybrid polymer fibers and investigated the behavior of rabbit fibroblasts cultured on these fibers. The objectives of this study were to determine the mechanical properties of the chitosan-based HA hybrid polymer fibers and to evaluate fibroblast adhesion, proliferation, and the synthesis of the ECM on the novel polymer fibers, and to show the superiority of the novel fiber as a scaffold biomaterial for ligament tissue engineering.

MATERIALS AND METHODS

Polymer fiber preparation

Polymer fibers were developed by the wet spinning method as described by Tamura and colleagues,[16] with the following modifications. Chitosan powder (Kimitu Chemical Co., Inc., Tokyo, Japan) was dissolved in 2% aqueous acetic acid to give a polymer concentration of 3.5%. The degree of deacetylation of the chitosan was 81%, and its viscosity average molecular weight was 600,000. The HA had a viscosity average molecular weight of 2,400,000, and was donated by Denki Kagaku Kougyo Co. Ltd. (Tokyo, Japan). The chitosan dope was spun into a calcium coagulant (64% $CaCl_2$ dissolved in 50% aqueous methanol solution) through a stainless steel spinneret (0.1 mm in diameter, 50 holes) at a winding speed of 4.2 m/min. A 50% aqueous methanol solution was used as the second coagulation bath, and 0.05% or 0.1% HA dissolved in 50% aqueous methanol solution was used as the third coagulation. All three coagulation baths were at room temperature. The resulting filaments were stretched at a ratio of 1.05 (4.5 m/min on the second roller : 4.2 m/min on the first roller) and treated with 0.8% sodium hydroxide dissolved in a 90% aqueous methanol solution. The fiber wound on the roller was washed in methanol and dried at room temperature. The diameter of each fiber was 0.03 mm. We prepared three types of fiber: a chitosan polymer fiber (chitosan group), and chitosan-based 0.05% HA hybrid fiber (ch/0.05HA group), and 0.1% HA hybrid fiber (ch/0.1HA group). In measuring the material properties and cell adhesion, polyglactin 910 (9-0 Vicryl suture material, Ethicon, Inc., NJ) was used as the control group. The diameter of this material is equal to that of the novel fibers. For their further investigations into cellular proliferation and ECM products, we made a fiber sheet using the original apparatus. Coagulated fibers were passed through a cross-feeding guide and wound onto a stainless roller (120 mm in diameter and 120 mm in width) at a rate of 17 rpm. The cross-feeding guide set forward of the roller was moved from side-to-side at a rate of 100 mm/30 s. The cross-feed length and rotation count were 100 mm and 40 times, respectively. The fibers wound onto the roller were washed and dehydrated with methanol, and then dried at room temperature. The dry filaments were cut from the roller and sheets of fiber filaments were piled 40 high (380 mm long × 100 mm wide × 0.25 mm thick). The sheets consisting of each polymer fiber were cut into small sheets and stacked in a perpendicular pattern of six layers (8 × 8 mm, 1-mm thick). A 2% chitosan gel was peripherally stuck onto each sheet and dried at 40°C overnight. Using this process, we constantly obtained the same 3D fabrications [Fig. 1(A, B)]: their porosity level was 200 μm. For the fibroblast culture, the 3D materials were sterilized in an autoclave at 135°C for 20 min.

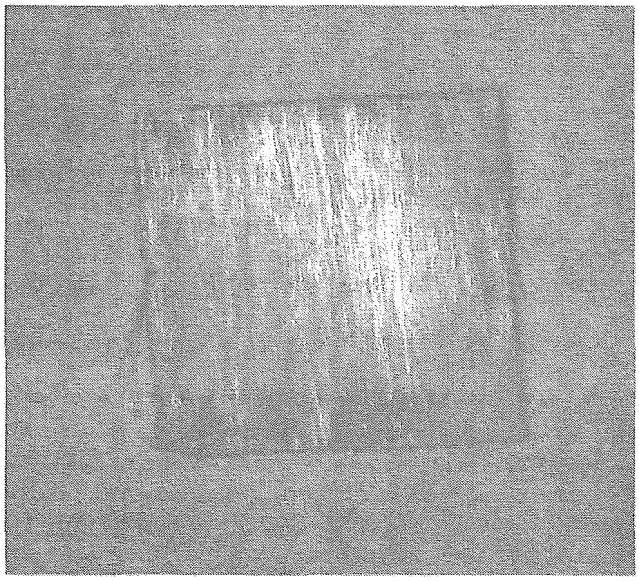

(A)

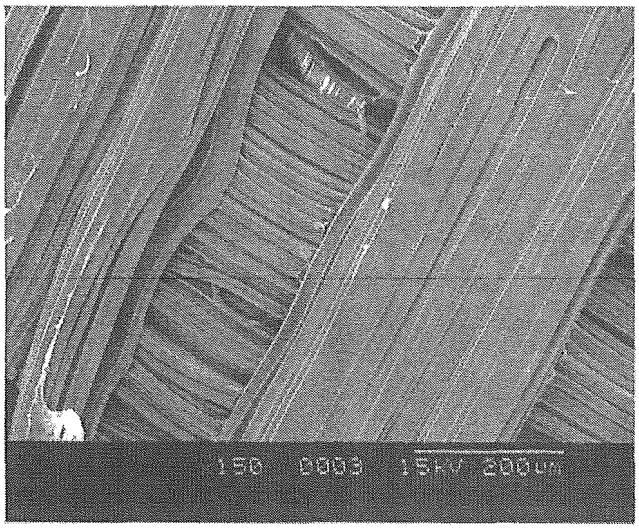

(B)

Figure 1. (A) Three-dimensional (3D) scaffold material for fibroblast culture. Sheets consisting of each polymer fiber were stacked in a perpendicular pattern of six layers (8 × 8 mm, 1 mm thick). (B) Scanning electron micrograph of 3D scaffold material.

Cell preparation

Fibroblasts were isolated from the patellar tendon substance of a Japanese white rabbit under sterile conditions, as described by Nagineni and colleagues.[17] The peritendinous tissues were carefully removed. Technically, patellar tendon is easier to manipulate compared to ligaments. Moreover, patellar tendon autograft has been clinically used as an autograft substitute for ligament reconstruction; therefore, we used the fibroblasts from the patellar tendon as the cell source. The culture medium used was Dulbecco's modified Eagle's medium (D5796, Sigma Chemical Co., St. Louis, MO), with 10% fetal bovine serum (10099-141, Invitrogen Corp., Carlsbad, CA), 10 μL/mL penicillin, streptomycin, and fungizone (17-745H, Biowhittaker, Walkersville, MD). The fibroblasts were incubated at 37°C in a humidified atmosphere of 5% CO_2 and supplemented with medium at 3-day intervals. Three weeks after culturing, the explanted pieces of patellar tendon were discarded and the outgrown cells were removed for subculture using trypsin. The fibroblasts were used at second passage in this study. The fibroblast suspension was concentrated to 1.4×10^7 cells/mL, counted using a hemocytometer, and fibroblast viability was more than 95%, as determined by the trypan blue indicator method.

Measurement of material properties

The material properties of each fiber were measured according to the Japanese Industrial Standards L1015 under dry conditions. To test the degradability of the hybrid fiber, the material properties of the ch/0.1HA group were evaluated after 0 and 2 h, and 14 and 28 days of incubation in the standard medium. Tensile tests for five samples of each material were performed at a crosshead speed of 20 mm/min using a material testing machine (P/N346-51299-02, Shimadzu, Kyoto, Japan). Each side of the fiber was nipped with a strip of a paper, and the fibers were mounted on the upper and lower chucks. The cross-sectional area was determined using a microscope (BX50, Olympus, Tokyo, Japan) and a video dimension analyzer (VM-30, Olympus, Tokyo, Japan). The load-deformation curve obtained from the testing machine was transferred to the stress–strain curve. Strain was defined as the increment of the grip-to-grip distance divided by the initial length. We confirmed that there was no slippage at the clamp.

Cell adhesion study

A cell adhesion study was performed as described in previous reports.[18,19] The fibrous samples were cut into 10-mm pieces and tightly packed into polytetrafluoroethylene tubes (30 mm in length, 7 mm in inner diameter; Sanplatec, Osaka, Japan). Each fibrous sample consisted of 1000 fibers. Then, 0.1 mL of fibroblast suspension (1.4×10^7 cells/mL) were loaded onto the column. The cells were allowed to adhere in a humidified incubator for 1 h. Each column was gently rinsed with 1 mL of 1 *M* phosphate-buffered saline per 30 s using a syringe and the number of unattached cells was quantified by the microscopic observation of the rinsed solution. Five samples in each group were measured.

Measurement of DNA content

A 50-μL aliquot of the fibroblast suspension (2.0×10^7 cells/mL) were loaded onto each 3D scaffold. After 1, 7, 14, and 28 days of culture, five of each fiber group were taken for analysis of DNA content to quantify cell proliferation.

DNA content was measured in aliquots of sodium citrate using a modified fluorometric assay with Hoechst dye 33258 (Polysciences Inc, Warrenton, PA).[20] The results of the DNA content assays were converted to cell numbers using a standard curve of control DNA (043-21751, Deoxyribonucleic Acid Sodium Salt from Salmon Spermary, Wako Pure Chemical Industries Ltd., Osaka, Japan).

Morphological and immunohistochemical analysis

After 14 days of culture, cell proliferation and ECM products were observed by light microscopy in the three types of 3D scaffold. In addition, scanning electron microscopy (SEM) observations were performed after 4 and 14 days of culture. For SEM observation, all samples were rinsed with Ringer's solution to remove nonattached cells. The cells on the scaffold were fixed overnight with 2.5% glutaraldehyde supplemented with 0.1 *M* phosphate buffer. After fixation, the SEM specimens were rinsed with phosphate buffer and fixed in 1% OsO_4 for 1 h, then soaked in 1% tannic acid for an additional hour. These procedures were repeated three times. The specimens were dehydrated, and mounted on an aluminum stub. They were coated with platinum palladuim in an argon atmosphere using an ion coater (E-1030, Hitachi, Tokyo, Japan) and then visualized by SEM (S-4500, Hitachi, Tokyo, Japan). After 14 days of culture, each specimen was also evaluated immunohistochemically for type I, type II, and type III collagen products. For immunohistochemical observation, the samples were stored in deep freeze conditions. Frozen sections (8-μm thick) were obtained to mount on microscope slides. Then, the sections were thawed and fixed with acetone for 5 min at −20°C. After drying, the sections were hydrated with phosphate-buffered saline for 5 min. After washing, the sections were stained with hematoxylin and eosin. They were incubated with the primary antibody — mouse monoclonal antibodies to either human collagen type I (1:100), type II (1:100), or type III (1:100, Fuji Chemicals, Takaoka, Japan) — for 60 min at room temperature. They were washed three times and incubated with a peroxidase-labeled polymer-conjugated anti-antibody (Envision System, Dako, CA) for 60 min. The reaction was developed with a 3,3'-diaminobenzidine tetrahydrochloride solution (DAB, Sigma Chemical, St Louis, MO).

Measurement of mRNA levels of ECM products in the implanted cells

To assess the mRNA levels of the ECM products in the implanted cells within the three types of 3D scaffolds, semi-quantitative reverse transcription-polymerase chain reaction (RT-PCR) analysis was performed, as described in a previous report.[21] The samples at 14 days after cultivation were obtained for this analysis. Before analysis, the samples were weighed and snap-frozen in liquid nitrogen. Relative band densities obtained in these manners were quantified using Quantity One® (PDI., Inc., Huntington Station, NY). Data were expressed as normalized ratios by comparing the integrated density values for the genes in question with the values for a housekeeping gene, glyceraldehydes-3-phosphate dehydrogenase (GAPDH), to yield a semi-quantitative assessment of gene expression.

TABLE I
Material Properties of Each Fiber

Material	Tensile Strength (MPa)	Strain at Failure (%)	Elastic Modulus (GPa)
Control	440.4 ± 13.8	30.4 ± 2.4	4.9 ± 0.4
Chitosan	128.1 ± 9.7[a]	4.3 ± 0.8[a]	7.8 ± 0.1[b]
Ch/0.05HA	152.6 ± 10.8[a,e]	6.1 ± 1.4[a]	6.9 ± 0.2[c]
Ch/0.1HA	217.6 ± 16.9[a,d,f]	3.2 ± 0.6[a,g]	11.8 ± 0.2[a,e,f]

[a]$p < 0.0001$ vs control group; [b]$p < 0.01$ vs control group; [c]$p < 0.05$ vs control group; [d]$p < 0.001$ vs chitosan group; [e]$p < 0.01$ vs chitosan group; [f]$p < 0.0001$ vs ch/0.05HA group; [g]$p < 0.01$ vs ch/0.05HA group.

$n = 5$, mean ± SD.

Control, polyglactin 910; ch/0.05 HA, chitosan-based 0.05% hyaluronan hybrid fiber; ch/0.1HA, chitosan-based 0.1% hyaluronan hybrid fiber.

Statistical analysis

Statistical comparisons were performed using one-way analysis of variance (ANOVA) and Fisher's PLSD post hoc test. The significant level was set at $p < 0.05$.

RESULTS

Material properties

All fibers failed at the midsubstance portion. Table I summarizes the material properties of each fiber. The mean tensile strength of the ch/0.1HA group was significantly greater than that of the chitosan and ch/0.05HA groups ($p < 0.0001$). However, the value of all the novel materials was significantly less than that of the control group ($p < 0.0001$). Strain at failure in the control group was significantly higher than that in the chitosan and hybrid groups ($p < 0.0001$). The stress–strain curves showed that the elastic modulus of the ch/0.1HA group was significantly higher than that of the control, chitosan, and ch/0.05HA groups [$p < 0.0001$; Fig. 2(A, B)]. The tensile strength of the ch/0.1HA group decreased with 2 h of incubation ($p < 0.001$); however, it was maintained during the period between 2 h and 28 days [Fig. 2(C)].

Cell adhesion

Figure 3 shows the number of unattached fibroblasts in the control and the three types of the novel

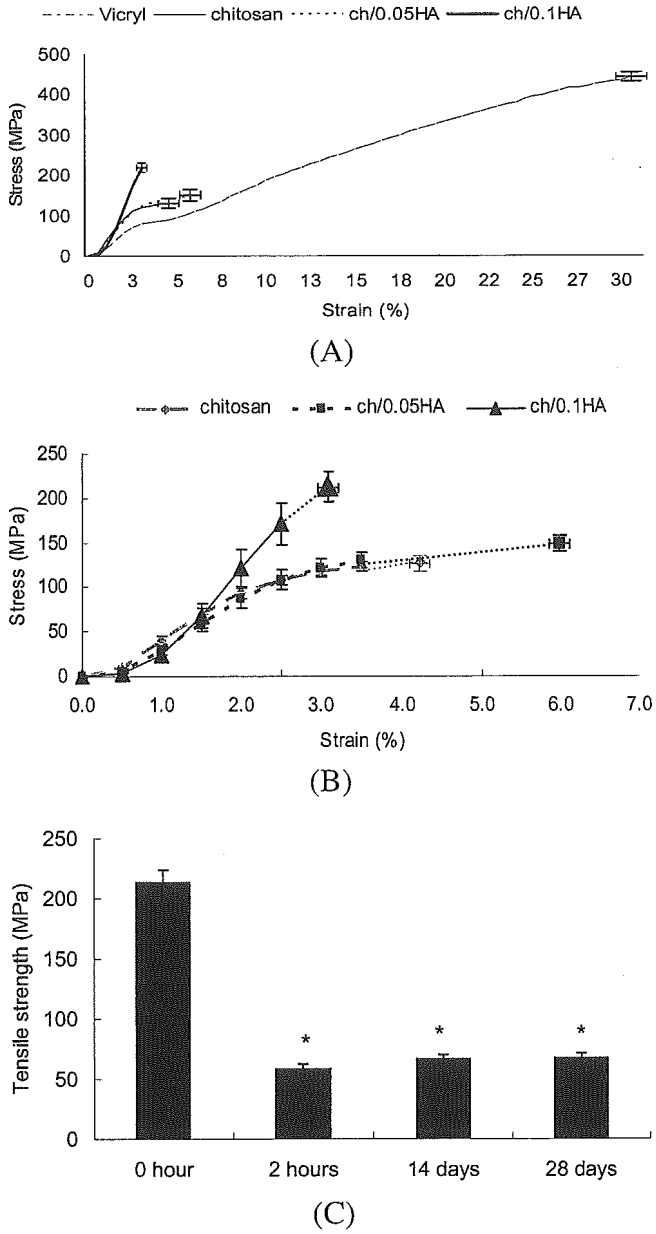

Figure 2. (A) Stress–strain curves of control, chitosan, ch/0.05HA, and ch/0.1HA group. (B) Enlarged view of (A). Ch/0.05HA, chitosan-based 0.05% hyaluronan hybrid fiber scaffold; ch/0.1HA, chitosan-based 0.1% hyaluronan hybrid fiber scaffold. Mean tensile strength and elastic modulus of ch/0.1HA group were significantly higher than those of chitosan and ch/0.05HA group. (C) Tensile strength of ch/0.1HA group decreased with 2 h of incubation; however, it was maintained during the period between 2 h and 28 days. * $p < 0.001$ vs 0 h.

fibers. The number of unattached fibroblasts in the chitosan and hybrid groups was significantly lower than in the control group ($p < 0.0001$). Moreover, HA hybridization significantly reduced the number of unattached fibroblasts ($p < 0.01$ vs chitosan group). However, there were no significant differences in the values between the ch/0.05HA and ch/0.1HA groups.

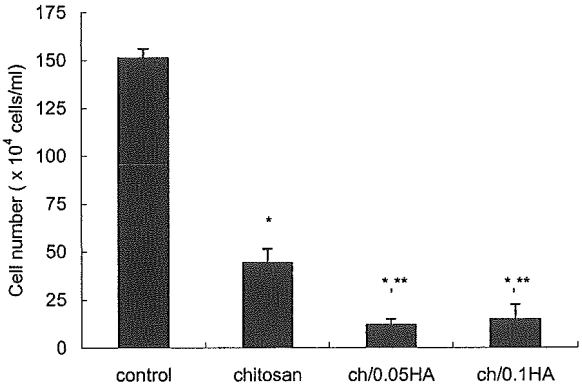

Figure 3. Number of fibroblasts unattached from control, chitosan, and chitosan-based hyaluronan hybrid polymer fibers. Hyaluronan coating reduced number of unattached cells. * $p < 0.0001$ vs control group. ** $p < 0.01$ vs chitosan group.

Cell proliferation

The light micrograph showed the proliferation of the fibroblasts on all of the fibers at 14 days after cultivation (Fig. 4). The SEM observation revealed that the number of fibroblasts increased from the 4th to 14th day of culture [Fig. 5(A, B)]. The amount of the DNA in each type of 3D scaffold increased with time (Fig. 6). Although the DNA content of the ch/0.1HA group was significantly higher than that of the chitosan group at 1 day after cultivation ($p < 0.05$), there were no significant differences in the values among the three groups at 7, 14, and 28 days after cultivation.

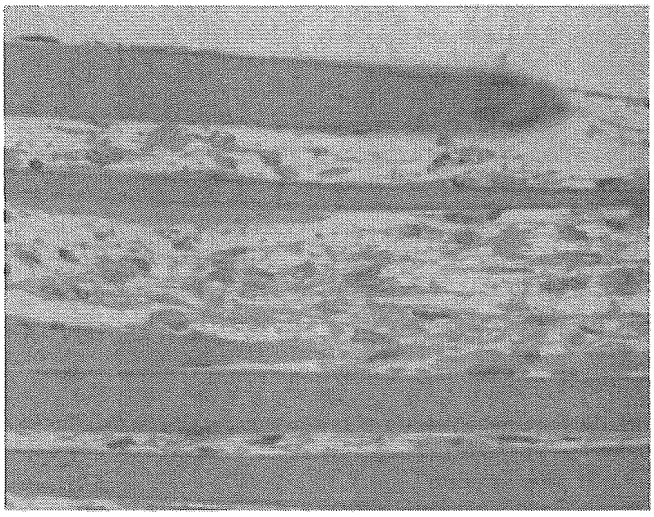

Figure 4. Light micrograph of fibroblasts proliferated in the 3D scaffold material consisting of the chitosan-based 0.1% hyaluronan hybrid polymer fiber at 14 days after cultivation (hematoxylin-eosin staining, original magnification, 400×). [Color figure can be viewed in the online issue, which is available at www.interscience.wiley.com.]

Cell morphology

The light micrograph (Fig. 4) and the SEM micrograph [Fig. 5(A)] disclosed that the fibroblasts were spindle-shaped, adhered to the polymer fibers, and the length of the cells were 20 to 50 μm. The existence or concentration of HA in the novel fiber did not affect the shape of implanted fibroblasts.

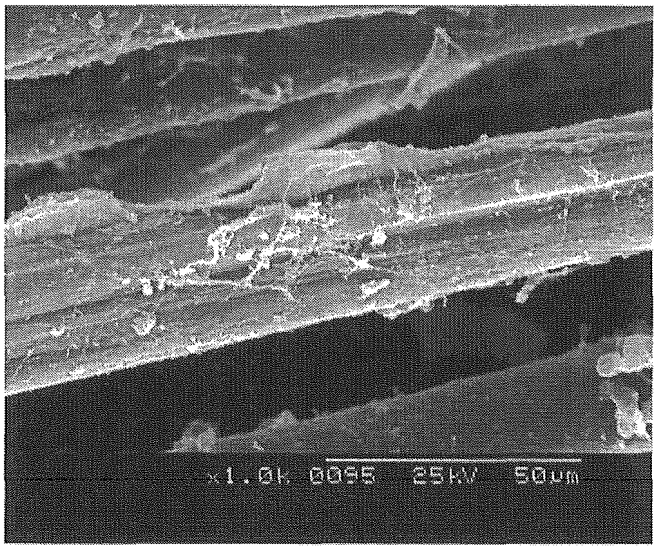

(A)

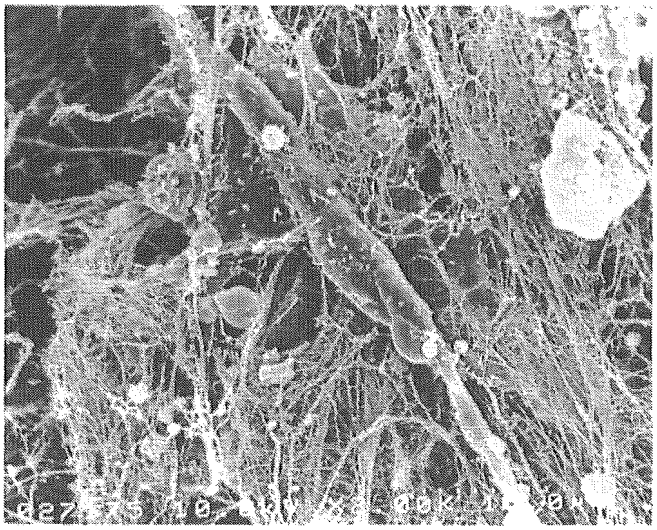

(B)

Figure 5. Scanning electron micrographs of chitosan-based 0.1% hyaluronan hybrid polymer fiber. (A) At 4 days after cultivation. Note that seeded fibroblasts were spindle-shaped and adhered to the polymer fibers (original magnification, 1000×). (B) At 14 days after cultivation. Note that synthesized collagen fibers were numerous around the polymer fibers and filled the interconnecting spaces. (original magnification, 2000×).

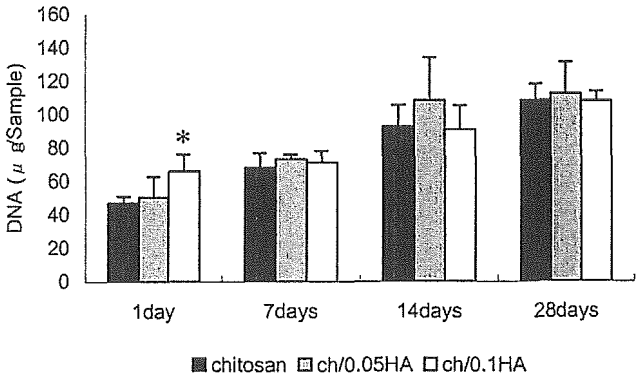

Figure 6. DNA content per sample (micrograms/sample) in cells retrieved from the chitosan and hybrid 3D scaffolds. In each type of 3D scaffold, the amount of the DNA increased with time. At 1 day after cultivation, DNA content of ch/0.1HA scaffold was higher than that of chitosan scaffold. * $p < 0.05$ vs chitosan scaffold.

Extracellular matrix (ECM) products

The SEM micrograph revealed that the seeded fibroblasts produced collagen fibrils onto the 3D polymer fiber scaffold at 4 days after cultivation [Fig. 5(A)]. At 14 days of culturing, the synthesized collagen fibers were numerous around the polymer fibers and filled the interconnecting spaces [Fig. 5(B)]. Immunostaining for type I collagen was prominent around the chitosan-based 0.1% HA hybrid fibers at 14 days after cultivation [Fig. 7(A)]. Type I collagen was more abundant around the surface of the fibers. On the other hand, type III collagen immunolabelling was not clearly detected around the fibers 14 days after cultivation [Fig. 7(B)]. There were no significant differences in staining among the three types of scaffolds. There was no staining for type II collagen around the fibers. Figure 8 shows the normalized ratios of matrix molecule mRNAs from fibroblasts in the three groups at 14 days after cultivation. The mRNA level of type I collagen in the ch/0.1HA group was significantly higher than in the other groups ($p < 0.01$ vs the chitosan group, $p < 0.05$ vs the ch/0.05HA group). Conversely, the level of type III collagen in the ch/0.1HA group was significantly less than in the chitosan and ch/0.05HA groups ($p < 0.01$ vs the chitosan group, $p < 0.01$ vs the ch/0.05HA group). Significant increases in the fibromodulin and biglycan mRNA levels were found in the HA hybrid fiber groups, compared with the chitosan group ($p < 0.01$). However, the data indicated that HA had no effect on the expression of decorin and lumican mRNAs.

DISCUSSION

Chitosan has been well accepted as a scaffold material in the field of musculoskeletal tissue engineer-

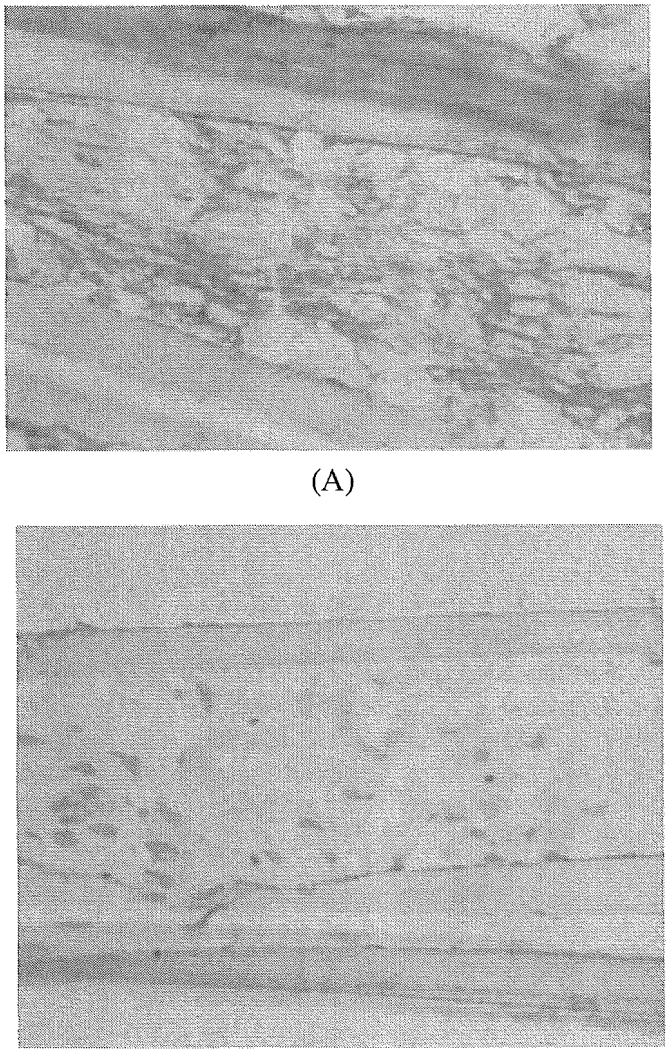

Figure 7. Immunostaining for type I and type III collagen in chitosan-based 0.1% hyaluronan hybrid polymer fibers at 14 days after cultivation. Type I collagen was more abundant, and type III collagen was not detected around fibers. (A) Type I collagen staining. (B) Type III collagen staining (original magnification, 400×). [Color figure can be viewed in the online issue, which is available at www.interscience.wiley.com.]

ing. Although several basic studies have demonstrated the tissue regeneration potential of GAG-augmented chitosan hydrogels,[22,23] these hydrogels do not have the required mechanical strength for use as a scaffold material for ligament tissue engineering. To overcome this limitation, we have developed a novel polymer fiber as a fundamental scaffold material for ligament regeneration. The present study showed that the chitosan-based HA hybrid polymer fibers had significantly higher mechanical strength, fibroblast adhesion, and ECM products, compared with nonhybrid chitosan fiber. These results indicate that HA enhances the mechanical strength of the polymer fibers and imparts superior biological effects on the fibroblasts in a 3D culture system.

Tamura and colleagues[16] reported that the enhancement of tensile strength was observed in chitosan-coated alginate filaments. Ionic interaction is the most convenient way to form tight interactions between two molecules. They stated that the tight interaction of chitosan with alginate increased the tensile strength of the hybrid fibers. In our novel hybrid fibers, chitosan is a cationic polysaccharide consisting of glucosamine residues and HA displays anionic behavior. Therefore, tight interaction between both molecules was expected, and the main reason for the increase in mechanical strength in the novel hybrid fiber is this tight interaction between chitosan and HA polymers. What is more important is to control the alteration of mechanical properties in the novel materials during the process of biodegradation. In general, the mechanical strength of fibers is higher under dry conditions than under wet conditions. Tamura and colleagues,[16] however, reported that their chitosan-coated alginate filaments showed higher strength under wet conditions. Although the tensile strength of this hybrid material decreased to one third of the initial strength at an early soaking time, this material maintained its tensile strength with up to 28 days of incubation. We obtained adequate mechanical strength of our novel hybrid fibers to create a 3D scaffold using the original apparatus. In addition, there is the possibility of maintaining adequate mechanical strength of implanted novel fibers *in vivo* until native ECM matures. This is the first report to reveal that the polyion complex effect of chitosan and HA was able to enhance the material properties of a fiber scaffold material.

In developing our novel biomaterial, the point we wish to emphasize is that our attempt is not only to increase the mechanical strength, but also to enhance the biological effects on the embedded cells. Chitosan is a partially deacetylated derivative of chitin, and the primary structural polymer in arthropod exoskeletons. The potential of chitosan as a biomaterial is based on its cationic nature and high-charge density in solution. The cationic nature of chitosan is considered to allow for electrostatic interactions with anionic GAGs and other negatively charged species.[24] These ionic interactions may serve as a mechanism for retaining and recruiting cells, growth factors, and cytokines within a scaffold. Based on this theoretical background, chitosan has been widely employed as an excellent biomaterial for wound healing and tissue repair applications. On the other hand, GAGs, which are part of the ECM components, play an important role in regulating expression of the cellular phenotype and in supporting tissue regeneration. Hyaluronan is the main component in the ECM of soft connective tissues.[25] A number of studies have shown the biological effects of HA on various cells.[11–14] In ligament

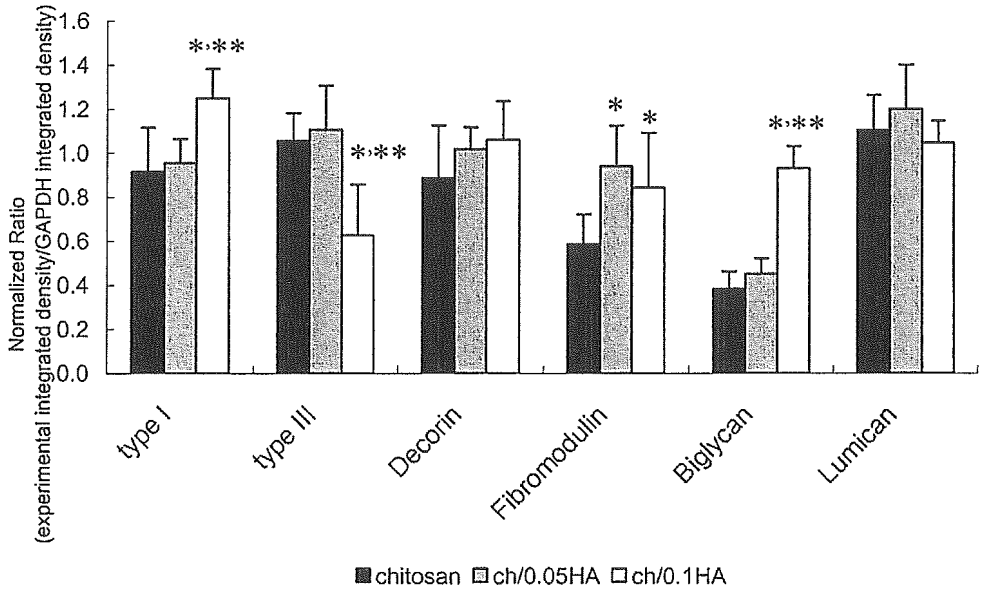

Figure 8. Normalized ratio (experimental integrated density/glyceraldehydes-3-phosphate dehydrogenase [GAPDH] integrated density) of mRNA for matrix molecules in fibroblasts after 14 days of culturing with chitosan, ch/0.05HA, and ch/0.1HA scaffold. Type I collagen mRNA level in ch/0.1HA were significantly higher in the chitosan and ch/0.05HA. On the other hand, type III collagen mRNA level in ch/0.1HA were significantly less than in the chitosan and ch/0.05HA. Type I, type I collagen; type III, type III collagen. * $p < 0.01$ vs chitosan group. ** $p < 0.05$ vs ch/0.05HA group.

tissue engineering, we should consider that the ligament is subject to excessive mechanical stress. To maintain the number of attached fibroblasts under these circumstances, highly cellular adhesivity is a requirement for ligament scaffold materials. Therefore, among the biological effects of HA, we focused especially on enhancing the cell adhesive potential of the novel material. Zimmerman and colleagues[26] showed that HA is an adhesion modulator molecule, which can mediate the early stage of cell–substrate interaction. Hu and colleagues[12] stated that HA material has positive advantages for fibroblast adhesion. Based on these previous data and the current results, it seems reasonable to conclude that scaffold biomaterials introducing HA provide excellent fibroblast adhesive activity.

CD44, a transmembrane glycoprotein expressed in a variety of cell types in connective tissues, is well known as the principal cell–surface receptor for HA.[27] The interaction of CD44 and HA plays a crucial role in regulating cellular activities, including cell–matrix adhesion, cell proliferation, cell migration, and ECM products. Murdoch and colleagues[28] demonstrated that there was a dramatic increase of CD44 expression in chondrocytes isolated from cartilage. As CD44 is a major cell-surface protein in fibroblasts,[29] the isolated fibroblasts from ligaments and tendons would increase in CD44 expression in a manner similar to chondrocytes. Although we did not clarify this point in the current study, the interaction of CD44 on the isolated fibroblast and HA on the scaffold material could provide excellent biological effects on the cultured fibroblast.

The optimum concentration of HA introduced to the novel material must be considered. In terms of cell adhesive potential, Zimmerman and colleagues[26] showed that excess HA on a substrate strongly inhibited cell adhesion. Huang-Lee and colleagues[30] stated that high concentration of HA served as a barrier interrupting direct communication between fibroblasts and ECM. These results indicate that the presence of a thin HA layer on a substrate increases the cell adhesive potential of materials. Based on this background, in the present study, we coated a relatively thin HA layer on the chitosan materials. The data obtained here agree with previous results.[11–14,26,30] However, we did not consider the optimum concentration of HA for enhancing the cell adhesive potential of the novel material. In a future study, this point must be determined.

In conclusion, this study reveals that HA hybridization of the fundamental scaffold material for ligament tissue engineering increases the mechanical strength and the biological effects on cultured fibroblasts. Although there are considerable limitations, the data derived from this study suggest that these novel hybrid fibers may become a useful material as a scaffold of ligament tissue engineering.

This work was supported by Grant-in-Aid for Science Research from Japanese Ministry of Education, Culture, Sports, Science & Technology (B-1539044) and Grant-in-Aid for New Energy and Industrial Technology Development Organization (03A04002a). The authors thank Mr. Tohru Mitsuno and Mr. Shouzou Miyoshi (General Research Center, Denki Kagaku Kougyou Co., Ltd., Tokyo, Japan) for their excellent technical assistance in fiber preparation.

References

1. Altman GH, Diaz F, Jakuba C, Calabro T, Horan RL, Chen J, Lu H, Richmond J, Kaplan DL. Silk-based biomaterials. Biomaterials 2003;24:401-416.
2. Awad HA, Boivin GP, Dressler MR, Smith FN, Young RG, Butler DL. Repair of patellar tendon injuries using a cell-collagen composite. J Orthop Res 2003;21:420-431.
3. Dunn MG, Liesch JB, Tiku ML, Zawadsky JP. Development of fibroblast-seeded ligament analogs for ACL reconstruction. J Biomed Mater Res 1995;29:1363-1371.
4. Gentleman E, Lay AN, Dickerson DA, Nauman EA, Livesay GA, Dee KC. Mechanical characterization of collagen fibers and scaffolds for tissue engineering. Biomaterials 2003;24: 3805-3813.
5. Quteish D, Singh G, Dolby AE. Development and testing of a human collagen graft material. J Biomed Mater Res 1990;24: 749-760.
6. Musahl V, Abramowitch SD, Gilbert TW, Tsuda E, Wang JH, Badylak SF, Woo SL. The use of porcine small intestinal submucosa to enhance the healing of the medial collateral ligament — a functional tissue engineering study in rabbits. J Orthop Res 2004;22:214-220.
7. Cao Y, Vacanti JP, Ma X, Paige KT, Upton J, Chowanski Z, Schloo B, Langer R, Vacanti CA. Generation of neo-tendon using synthetic polymers seeded with tenocytes. Transplant Proc 1994;26:3390-3392.
8. Ibarra C, Cao Y, Kim TH. Tissue engineering ligaments. Surg Forum 1996;47:612-615.
9. Langer R, Vacanti JP. Tissue engineering. Science 1993;260: 920-926.
10. Hynes RO. Cell adhesion: old and new questions. Trends Cell Biol 1999;9:M33-M37.
11. Roy F, DeBlois C, Doillon CJ. Extracellular matrix analogs as carriers for growth factors: in vitro fibroblast behavior. J Biomed Mater Res 1993;27:389-397.
12. Hu M, Sabelman EE, Lai S, Timek EK, Zhang F, Hentz VR, Lineaweaver WC. Polypeptide resurfacing method improves fibroblast's adhesion to hyaluronan strands. J Biomed Mater Res 1999;47:79-84.
13. Huang L, Cheng YY, Koo PL, Lee KM, Qin L, Cheng JC, Kumta SM. The effect of hyaluronan on osteoblast proliferation and differentiation in rat calvarial-derived cell cultures. J Biomed Mater Res 2003;66:880-884.
14. Lokeshwar VB, Iida N, Bourguignon LYW. The cell adhesion molecule, GP116, is a new CD44 variant (ex14/v10) involved in hyaluronic acid binding and endothelial cell proliferation. J Biol Chem 1996;271:23853-23864.
15. Malette WG, Quigley HJ, Gaines RD, Johnson ND, Rainer WG. Chitosan: a new hemostatic. Ann Thorac Surg 1983;36:55-58.
16. Tamura H, Tsuruta Y, Tokura S. Preparation of chitosan-coated alginate filament. Mater Sci Eng C 2002;20:143-147.
17. Nagineni CN, Amiel D, Green MH, Berchuck M, Akeson WH. Characterization of the intrinsic properties of the anterior cruciate and medial collateral ligament cells: an in vitro cell culture study. J Orthop Res 1992;10:465-475.
18. Nishimura S, Nishi N, Tokura S. Adhesion behavior of murine lymphocytes on the surface of fibrous chitin and its derivatives. Int J Biol Macromol 1985;7:100-104.
19. Iwasaki N, Yamane ST, Majima T, Kasahara Y, Minami A, Harada K, Nonaka S, Maekawa N, Tamura H, Tokura S, Shiono M, Monde K, Nishimura S. Feasibility of polysaccharide hybrid materials for scaffolds in cartilage tissue engineering: evaluation of chondrocyte adhesion to polyion complex fibers prepared from alginate and chitosan. Biomacromolecules 2004;5:828-833.
20. Kim YJ, Sah RL, Doong JY, Grodzinsky AJ. Fluorometric assay of DNA in cartilage explants using Hoechst 33258. Anal Biochem 1988;174:168-176.
21. Majima T, Marchuk LL, Sciore P, Shrive NG, Frank CB, Hart DA. Compressive compared with tensile loading of medial collateral ligament scar in vitro uniquely influences mRNA levels for aggrecan, collagen type II, and collagenase. J Orthop Res 2000;18:524-531.
22. Sechriest VF, Miao YJ, Niyibizi C, Westerhausen-Larson A, Matthew HW, Evans CH, Fu FH, Suh JK. GAG-augmented polysaccharide hydrogel: a novel biocompatible and biodegradable material to support chondrogenesis. J Biomed Mater Res 2000;49:534-541.
23. Suh JK, Matthew HW. Application of chitosan-based polysaccharide biomaterials in cartilage tissue engineering: a review. Biomaterials 2000;21:2589-2598.
24. Madihally SV, Matthew HW. Porous chitosan scaffolds for tissue engineering. Biomaterials 1999;20:1133-1142.
25. Laurent TC, Fraser JR. Hyaluronan. FASEB J 1992;6:2397-2404.
26. Zimmerman E, Geiger B, Addadi L. Initial stages of cell-matrix adhesion can be mediated and modulated by cell-surface hyaluronan. Biophys J 2002;82:1848-1857.
27. Underhill, C. CD44: the hyaluronan receptor. J Cell Sci 1992; 103:293-298.
28. Murdoch AD, Oldershaw RA, Hardingham TE. Differential regulation of cell-surface proteoglycans by chondrocytes during adaptation to cell culture. Ann Meeting Orthop Res Soc 2003;No. 0220.
29. Holifield BF, Jacobson K. Mapping trajectories of Pgp-1 membrane protein patches on surfaces of motile fibroblasts reveals a distinct boundary separating capping on the lamella and forward transport on the retracting tail. J Cell Sci 1991;98:191-203.
30. Huang-Lee LL, Wu JH, Nimni ME. Effects of hyaluronan on collagen fibrillar matrix contraction by fibroblasts. J Biomed Mater Res 1994;28:123-132.

Hand Surgery, Vol. 10, No. 1 (July 2005) 77–82

World Scientific
www.worldscientific.com

A LONG-TERM FOLLOW-UP OF SILICONE-RUBBER INTERPOSITION ARTHROPLASTY FOR OSTEOARTHRITIS OF THE THUMB CARPOMETACARPAL JOINT

Akio Minami, Norimasa Iwasaki, Keiji Kutsumi, Naoki Suenaga and Kazunori Yasuda

Department of Orthopaedic Surgery
Hokkaido University School of Medicine
Sapporo, 060-8638, Japan

Received 18 August 2004; Accepted 13 June 2005

ABSTRACT

There are several surgical options for osteoarthritis (OA) of the thumb carpometacarpal (CMC) joint. This paper presents our long-term clinical and radiographic review of 12 thumbs in ten patients treated by partial trapezial excision and silicone-rubber interposition arthroplasty. The follow-up period averaged 15; three years with a ten-year minimum. Although the procedure provided early pain relief in most thumbs, all but two had mild to severe pain at follow-up. The average range of post-operative palmar abduction was 23°. The average post-operative grip strength was 9.5 kg. Both tip and key pinch between thumb and index finger averaged about 50% that of normal subjects. Dislocation of the implant occurred in two joints and breakages in five. Bony erosions around the implant, which we attributed silicone synovitis, were found in four thumbs. The indications for silicone-rubber interposition arthroplasty for OA of the thumb CMC joint should be severely restricted as these produced unsatisfactory long-term results.

Keywords: Silicone-Rubber Interposition Arthroplasty; Osteoarthritis; Carpometacarpal Joint; Thumb; Silicone Synovitis.

INTRODUCTION

Osteoarthritis (OA) of the carpometacarpal (CMC) joint is a common cause of pain at the base of the thumb, which can seriously impair overall hand function. Motion, primarily in radial and palmar abduction of the thumb is often limited; and grip and pinch strengths are diminished because of pain or subluxation of the CMC joint.

Surgical treatment options include trapezial excision,[1–3] trapeziometacarpal arthrodesis,[4–6] metalloplastic arthroplasty,[7–11] ligament reconstruction with tendon interposition,[12–16] and silicone arthroplasty.[17–23] Silicone arthroplasties may be accomplished by two means. Swanson developed a silicone implant with a stem for insertion in the first metacarpal intramedullary cavity. It had a smooth proximal enlargement that filled the space produced by trapezial excision and articulated with the scaphoid.[22,23] There have been several reports of the efficacy of this procedure. They show mixed results.[18,20,24] Subluxation and implant failures due to fracture or silicone synovitis are major concerns.[21,24] These failures have required implant removal and synovectomy.[24]

Ashworth *et al.* developed an interposition (button) silicone-rubber arthroplasty.[17] There are only a few reports on the long-term results of this procedure.[17,20]

Correspondence to: Dr. Akio Minami, Department of Orthopaedic Surgery, Hokkaido University School of Medicine, Kita-15-jo, Nishi-7-chome, Kita-ku, Sapporo 060-8538, Japan.Tel: (+81) 11-706-5933, Fax: (+81) 11-717-3532, E-mail: a-minami@med.hokudai.ac.jp

The purpose of this study is to determine the advantages, disadvantages and indications of the procedure, by reviewing the long-term clinical and radiographic results of surgery performed more than ten years ago.

MATERIALS AND METHODS

A total of 12 silicone interposition arthroplasty procedures at the CMC joint of the thumb were performed on ten patients after 1978.[17] Five procedures were performed on the right hand, three on the left, and four were bilateral. There were eight female and two male patients with an average age at the time of operation of 66 years (range, 53 to 79 years). All patients received conservative therapy, including intra-articular corticosteroids and immobilisation for varying periods of time in the year prior to operation. The follow-up period ranged from ten years and one month to 21 years (average, 15 years and four months) (Table 1).

Clinical results are rated as excellent, good, fair, and poor. Excellent means that abduction of the thumb and grip strength were maintained or increased without pain. Good means a minimal decrease in abduction and grip strength or there was mild residual pain. Fair means that either grip strength or abduction was maintained but there was pain limiting function. Poor means a loss of abduction and grip strength and pain limiting function.

We evaluated the clinical results on the following criteria: pain, range of motion (maximum palmar abduction and adduction), grip strength, pinch strength (tip and key), vocational status, patient satisfaction and 14 activities of daily living. Pain was graded as no pain, mild (no effect on activity), moderate (affects activity), and severe (frequent pain with light activity).

Palmar abduction and adduction were measured on X-ray films. The thumb was palmarly abducted 45° from the axis formed by the metacarpal heads of the index and middle fingers. An X-ray film was placed parallel to the surface formed between the thumb and index finger (Fig. 1). The films were then exposed. The thumb was maximally palmarly abducted and adducted. Then the angles between the longitudinal axes of the metacarpals of the thumb and index fingers, defined as angles of maximum abduction and adduction of the thumb, were measured.

Tip pinch and key pinch between the thumb and index finger, and grip strength were recorded with a Green Leaf Medical pinch-meter and a Jamar dynamometer, respectively (EUAL; Green Leaf Medical Systems, Palo Alto, CA) according to the protocol described by Mathiowetz *et al.*[25]

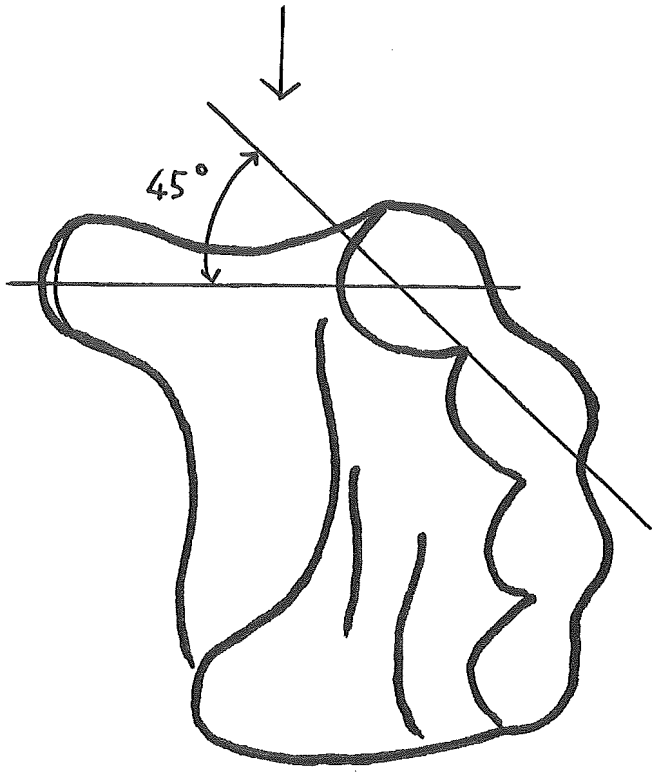

Fig. 1 Palmar abduction and adduction were measured on X-ray films. The thumb was palmarly abducted 45° from the axis formed by the metacarpal heads of the index and middle fingers. An X-ray film was placed parallel to the surface formed between the thumb and index finger.

Function was assessed on the patient's ability to perform several activities of daily living including writing, light housework, opening a car door, turning a key, and opening a jar.

Radiographically, there were varying degrees of flattening of the distal radial wedge of the trapezium, subluxation of the first metacarpal, osteophyte formation, osteosclerosis, and joint space narrowing. There was mild degeneration of the scaphotrapezial joint in four joints. The radiographic findings were classified into four stages according to Eaton's classification.[13] We determined that one joint was in stage II, seven in stage III, and four in stage IV.

SURGICAL TECHNIQUES

The CMC joint of the thumb is exposed through a dorsal curved longitudinal incision. The abductor pollicis longus tendon is detached at its insertion, and the extensor pollicis brevis tendon

is retracted. Osteophytes around the CMC joint, in particular, medial osteophytes are removed.

A power drill is used to create a crater 5 to 7 mm wide in the distal surface of the body of the trapezium. The depth of the crater is adjusted to accept the stem of the trapezial implant. Prior to final insertion, the disc portion of the implant is trimmed to the diameter of the distal surface of the trapezium.

As the metacarpal is maintained in reduced alignment with the trapezium, the abductor pollicis longus tendon is advanced distally on the base of the metacarpal for re-insertion. The capsule is tightly closed and then reinforced with additional sutures along both sides of the abductor pollicis longus.

When an accessory slip of the abductor pollicis longus tendon is present, it may be used for reinforcement of the capsule. The tendon slip is divided 3 cm proximal to its insertion into the fascia of the abductor pollicis brevis muscle. The distal portion is re-routed distally over the capsule of the CMC joint, beneath the extensor pollicis longus and brevis tendons, and inserted into the periosteum of the second metacarpal with a pull-out suture.

A palmar plaster splint maintains the thumb in the abducted position. Occasionally, two small Kirschner wires are placed at an oblique angle between the first and second metacarpals to provide stabilisation. The dressing and splint are removed in about ten days, and a thumb spica cast is applied for an additional four to five weeks. Following removal of the cast, active range of motion exercises is permitted.

RESULTS

Clinical Results

Overall, clinical results were rated as good in two, fair in two, and poor in eight. There were no excellent results (Table 1).

Pain All patients complained of pain before surgery (ten severe and two moderate). The severity of the pain improved in all patients immediately after surgery. At final follow-up, two had complete relief of pain; one had mild pain, two had moderate pain, and seven had severe pain. Pain was elicited mainly by maximum palmar and radial abduction.

Motion After silicone interposition arthroplasty maximum palmar abduction averaged 38.8° ± 1.1° and maximum adduction averaged 16.3° ± 1.4°. The average range of motion was 22.5° ± 1.8°.

Grip Strength All patients had OA of the CMC joint of the contralateral thumbs in the cases that a unilateral arthroplasty

Table 1 Data of all Patients (1).

Case No.	Sex Age (Yrs)	Stage*	Follow-up (Yrs.+mths)	Post-operative Results		
				Pain	Subluxation (%)†	Implant Failure
1	M‡, 73	IV	16 + 1	Moderate	29	
	79	II	10 + 1	Severe	25	Silicone synovitis
2	F§, 61	III	16 + 3	Severe	20	Dislocation
3	M, 72	III	17 + 4	Mild	40	
4	F, 55	III	21 + 0	No	23	Breakage + Silicone synovitis
	56	III	20 + 5	Severe	36	Dislocation
5	F, 76	IV	17 + 1	Moderate	25	
6	F, 65	III	15 + 11	Severe	23	Breakage
7	F, 73	III	11 + 6	No	25	Breakage
8	F, 77	IV	10 + 6	Severe	35	
9	F, 53	III	13 + 8	Severe	40	Breakage + Silicone synovitis
10	F, 54	IV	14 + 5	Severe	35	Breakage + Silicone synovitis

*Stage was classified by Eaton's classification.

†The degree of the subluxated metacarpal was expressed as a percent age divided by the width of the distal articular surface of the trapezium.

‡M : Male.

§F : Female.

Table 1 (*Continued*)

Case No.	Post-operative Clinical Results: Maximum Abduction (Degrees)	Maximum Addution (Degrees)	Range of Motion	Grip Strength (kgf) Pre-/Post-operative	Tip Pinch (kgf)	Key Pinch (kg)	Overall Clinical Results
1	35	10	25	15/15	1.7	2.5	Fair
	35	15	20	20/13	2.8	3.8	Poor
2	40	10	30	10/7	2.5	3.0	Poor
3	40	15	25	9/10	3.7	4.1	Fair
4	35	15	20	12/8	5.0	2.4	Good
	40	10	30	12/10	3.4	2.5	Poor
5	35	25	10	8/5	2.2	3.4	Poor
6	45	15	30	10/7	3.9	3.4	Poor
7	45	20	25	9/9	3.5	3.2	Good
8	40	20	20	12/8	3.0	3.2	Poor
9	35	20	15	12/10	3.4	3.8	Poor
10	40	20	20	15/12	3.2	3.8	Poor

had been performed. Therefore, it was meaningless to compare the operated with the unoperated side. Pre-operative grip strength of the operated side averaged 12.0 ± 1.0 kg. After surgery the average grip strength decreased to 9.5 ± 0.8 kg. Only one patient had increased grip strength over the pre-operative value, two were unchanged and nine had decreased grip strength.

Tip and Key Pinches Post-operative tip pinch strength between the thumb and index finger averaged 3.2 ± 0.2 kg (range, 1.7–5.0). Key pinch strength averaged 3.2 ± 0.2 kg (range, 2.5–4.1). In normal comparable subjects tested in our department, tip pinch strength averaged 6.2 kg and key pinch strength averaged 6.8 kg. Therefore, the pinch strengths after silicone interposition arthroplasty were about 50% of normal subjects.

Patient Satisfaction Three patients were satisfied with the post-operative clinical results; however, seven patients were dissatisfied due to persistent pain and difficulties with the activities of daily living.

Performance of Activities of Daily Living Fourteen subjects were examined on the activities of daily living, post-operatively. The number of patients who complained of difficulty or incapability in each subject is shown in Fig. 2. The tests in which the patient complained of difficulty to perform are mainly associated with grasping and twisting small objects.

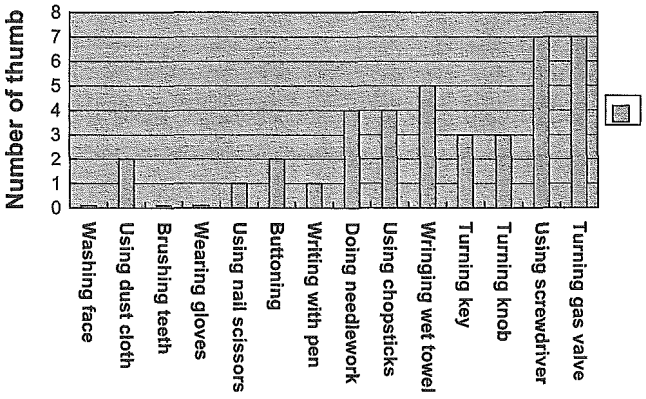

Fig. 2 Performance of activities of daily living. Fourteen subjects were examined on the activities of daily living, post-operatively. The number of patients who complained of difficulty or incapability in each subject is shown.

Return to Work The patients' pre-operative occupations were considered to have low demand activities. Post-operatively all the patients were retired males or homemakers. Therefore, all patients returned to work demands similar to their pre-operative status.

Radiographic Results

There were no cases without radiographic complications. The proximal bases of the first metacarpals were subluxed

palmarward in all thumbs. The degree of the metacarpal subluxatation was expressed as a percentage where the contact distance between metacarpal base and traperzium was divided by the width of the distal articular surface of the trapezium. The degree of subluxation of the metacarpal base ranged from 20% to 40% with an average of 29.7% (2.1).

Post-operative Complications

There were several post-operative complications of the implant. The implant broke in five thumbs and dislocated in two. Those were detected by direct vision and on X-ray film. Silicone synovitis was detected in four wrists clinically and radiographically. Secondary arthrodeses were performed in two patients, one between scaphoid and first metacarpal base, and the other between the first and second metacarpals, trapezoid and remaining trapezium using an iliac bone graft. The other refused further operation.

DISCUSSION

There are many options for surgical treatment of OA of the CMC joint of the thumb.[3–9,11,12,14–18,20–23] Each of the techniques has advantages and disadvantages.

Successful fusion permits good strength of grip and relief of pain, but decreases mobility. Hyper-extension of the metacarpophalangeal joint and OA of the scaphotrapeziotrapezoidal joint frequently occurred after CMC joint fusion. The removal of the trapezium reduces grip strength. Recently, most hand surgeons prefer to use trapeziectomy with ligament reconstruction rather than arthrodesis of the CMC joint.[12] Downing and Davis investigated trapezial space height after trapeziectomy.[26] Their patients were randomly allocated to treatment by either trapeziectomy alone or trapeziectomy with tendon interposition or ligament reconstruction. The post-operative trapezial space ratio decreased significantly from the pre-operative ratio in all three procedures. There was no significant difference between these one-year follow-up trapezial space ratios.

Swanson reported that replacing the trapezium with a silicone implant provides good range of motion and grip strength.[22] Previous reports of silicone arthroplasty show mixed results.[21,24] Implant failures because of fracture and resultant silicone synovitis are major concerns.[20,25] Bezwada *et al.* evaluated the long-term results of CMC joint silicone arthroplasty.[18] Sixty-two implants were available for follow-up evaluation at an average 16.4 years. They concluded that silicone arthroplasty seems to be a reliable option for disabling CMC joint arthritis and is associated with a high degree of patient satisfaction. Filling of the resected joint area with tendon tissue as an alternative to silicone has been reported to provide good results.[27,28]

Ashworth *et al.* first reported short-term results of silicone-rubber interposition arthroplasty using a modified silicone neurosurgical burr-hole cover in 42 patients.[17] The average follow-up time was 31 months. Forty results were rated as excellent. There were only two failures due to breakage of the device, and in both cases the breakage was due to a technical error. Oka and Ikeda described clinical and radiographic results of OA of the CMC joint of the thumb treated by Ashworth's technique with an average follow-up of 4.5 years.[20] Partial failure of the implant was seen in five of 16 patients. Three of the five cases merely complained of strange sensations and did not have pain, reduced grip strength, or difficulty with daily living activities. They found that the implant had subsided in three patients. Although two of the patients sometimes complained of pain, it was milder and much less than that experienced before surgery. Therefore, they emphasised that the development of pain was not always consistent with implant abnormality.

On the other hand, this long-term follow-up study has results quite different from Ashworth *et al.*'s and Oka and Ikeda's reports.[17,20] In spite of providing early pain relief in most thumbs, all but two thumbs had mild to severe pain at follow-up. Most patients complained of torsional pain or weakness when they grasped or pinched items. Dislocations of the implant occurred in two joints and implant breakages in five. Bony erosions thought to be silicone synovitis, were found around the implant in four thumbs.

Although two previous reports found no correlation between clinical results and roentgenographic findings,[21,28] our results show a significant correlation between poor clinical results and disintegration of the silicone implants.

We concluded that the Ashworth silicone interposition arthroplasty for OA of the thumb CMC joint produced unsatisfactory results and the indication for further use should be severely restricted.

ACKNOWLEDGEMENTS

The authors thank Ronald L. Linscheid, MD, Professor Emeritus, Surgery of the Hand, Department of Orthopedics, Mayo Clinic,

Rochester MN, USA, for his suggestion and advice during this investigation.

References

1. Gervis WH, A review of excision of the trapezium for osteoarthritis of the trapezio-metacarpal joint after twenty years, *J Bone Joint Surg* **55B**: 56–57, 1973.
2. Gervis WH, Wells T, Excision of the trapezium for osteoarthritis of the trapezio-metacarpal joint, *J Bone Joint Surg* **31B**:537–539, 1949.
3. Murley AHG, Excision of the trapezium in osteoarthritis of the first carpo-metacarpal joint, *J Bone Joint Surg* **42B**: 502–507, 1960.
4. Bamberger HB, Stern PJ, Kiefhaber TR, McDonough JJ, Cantor RM, Trapeziometacarpal joint arthrodesis: a functional evaluation, *J Hand Surg* **17A**:605–611, 1992.
5. Carroll RE, Hill NA, Arthrodesis of trapeziometacarpal joint of the thumb, *J Bone Joint Surg* **55B**:292–294, 1973.
6. Muller GM, Arthrodesis of the trapezio-metacarpal joint for osteoarthritis, *J Bone Joint Surg* **31B**:540–541, 1949.
7. Boeckstyns MEH, Sinding A, Elholm KT, Rechnagel K, Replacement of the trapeziometacarpal joint with a cemented (Caffiniere) prosthesis, *J Hand Surg* **14A**:83–89, 1989.
8. Braun RM, Total joint arthroplasty at the carpometacarpal joint of the thumb, *Clin Orthop* **195**:161–167, 1985.
9. Cooney WP, Linscheid RL, Askew LJ, Total arthroplasty of the thumb trapeziometacarpal joint, *Clin Orthop* **220**:35–45, 1987.
10. Ferrari B, Steffee AD, Trapeziometacarpal total joint replacement using the Steffee prosthesis, *J Bone Joint Surg* **68A**:1177–1184, 1986.
11. Wachtl SW, Sennwald GR, Non-cemented replacement of the trapeziometacarpal joint, *J Bone Joint Surg* **78B**:787–792, 1996.
12. Burton RI, Pellegrine VD Jr, Surgical management of basal joint arthritis of the thumb. Part II. Ligament reconstruction with tendon interposition arthroplasty, *J Hand Surg* **11A**:324–332, 1986.
13. Eaton RG, Littler JW, Ligament reconstruction for the painful thumb carpometacarpal joint, *J Bone Joint Surg* **55A**:1655–1666, 1973.
14. Lins RE, Gelberman RH, McKeown L, Katz JN, Kadiyala RK, Basal joint arthritis: trapeziectomy with ligament reconstruction and tendon interposition arthroplasty, *J Hand Surg* **21A**:203–209, 1996.
15. Tomaino MM, Pellegrini VD Jr, Burton RI, Arthroplasty of the basal joint of the thumb: long-term follow-up after ligament reconstruction with tendon interposition, *J Bone Joint Surg* **77A**:346–355, 1995.
16. Weilby A, Tendon interposition arthroplasty of the first carpometacarpal joint, *J Hand Surg* **13B**:421–425, 1988.
17. Ashworth CR, Blatt G, Chuinard RG, Stark HH, Silicone-rubber interposition arthroplasty of the carpometacarpal joint of the thumb, *J Hand Surg* **2**:345–357, 1977.
18. Bezwada MP, Sauer ST, Hankins ST, Wabber JB, Long-term results of trapeziometacarpal silicone arthroplasty, *J Hand Surg* **27A**:409–417, 2002.
19. Eaton RG, Replacement of the trapezium for arthritis of the basal articulations, *J Bone Joint Surg* **61A**:76–82, 1979.
20. Oka Y, Ikeda M, Silastic interposition arthroplasty for osteoarthritis of the carpometacarpal joint of the thumb, *Tokai J Exp Clin Med* **25**:15–21, 2000.
21. Pellegrini VD Jr, Burton RI, Surgical management of basal joint arthritis of the thumb. Part I. Long-term results of silicone implant arthroplasty, *J Hand Surg* **11A**:309–324, 1986.
22. Swanson AB, Disabling arthritis at the base of the thumb, *J Bone Joint Surg* **54A**:456–471, 1972.
23. Swanson AB, Swanson GD, Watermeier JJ, Trapezium implant arthroplasty. Long-term evaluation of 150 cases, *J Hand Surg* **6**:125–141, 1981.
24. Jennings CD, Livingstone DP, Convex condylar arthroplasty of the basal joint of the thumb: failure under load, *J Hand Surg* **15A**:573–581, 1990.
25. Mathiowetz V, Weber K, Volland G, Kashman N, Reliability and validity of grip and pinch strength evaluation, *J Hand Surg* **9A**:222–226, 1984.
26. Downing ND, Davis TRC, Trapezial space height after trapeziectomy: mechanism of formation and benefits, *J Hand Surg* **26A**:862–868, 2001.
27. Menon J, Schoene HR, Hohl JC, Trapeziometacarpal arthritis, Results of tendon interposition arthroplasty, *J Hand Surg* **6**:442–446, 1981.
28. Momose T, Nakatsuchi Y, Saito K, Hosaka M, Kitagawa K, Follow-up study of tendon interposition arthroplasty for osteoarthritis of the carpometacarpal joint of the thumb, *J Jap Soc Surg Hand* **8**:742–745, 1991.

Patterns of Carpal Deformity in Scaphoid Nonunion: A 3-Dimensional and Quantitative Analysis

Kunihiro Oka, MD, Hisao Moritomo, MD, PhD,
Tsuyoshi Murase, MD, PhD, Akira Goto, MD,
Kazuomi Sugamoto, MD, PhD, Hideki Yoshikawa, MD, PhD, *Osaka, Japan*

Purpose: To clarify quantitatively the 3-dimensional deformity of the carpus in scaphoid nonunion on the basis of fracture location.

Methods: Three-dimensional computed tomography was used to examine 20 patients with scaphoid nonunion. Displacements of the distal and proximal fragments of the scaphoid, lunate, triquetrum, and capitate were visualized and quantified using a 3-dimensional image-matching technology. Cases were categorized as distal fracture (16 cases) or proximal fracture (4 cases) based on the location of the fracture line relative to the dorsal apex of the scaphoid ridge where the dorsal scapholunate interosseous ligament is attached.

Results: The displayed distal scaphoid fractures showed that the proximal fragment of the scaphoid, lunate, and triquetrum rotated into extension and supination. The distal fragment of the scaphoid and capitate translated dorsally without notable rotation. The deformity in proximal fractures was less remarkable than that in distal fractures. Most distal scaphoid nonunions had dorsal intercalated segment instability deformity patterns, whereas a dorsal intercalated segment instability occurred in only 1 case of a proximal fracture.

Conclusions: Whether the fracture line passes distal or proximal to the dorsal apex of the scaphoid determines the subsequent carpal deformity. Dorsal translation of the distal fragment might be one of the factors in the development of degenerative change at the radial styloid. (J Hand Surg 2005; 30A:1136–1144. Copyright © 2005 by the American Society for Surgery of the Hand.)

Type of study/level of evidence: Prognostic, Level II.

Key words: Scaphoid nonunion, carpal deformity, natural history, degenerative arthritis, fracture location.

It has been proposed that long-standing untreated scaphoid nonunion leads to carpal collapse and subsequent degenerative arthritis of the wrist.[1–7] It generally is believed that the deformity associated with scaphoid nonunion starts as erosion of the palmar ulnar cortexes at a fracture site[2] followed by angulated deformity of the 2 fragments at the scaphoid nonunion and dorsal rotation of the lunate, which is referred to as dorsal intercalated segment instability (DISI) deformity. Eventually degenerative changes are observed first between the distal scaphoid and the radial styloid articular surfaces and develop progressively.[8,9] These deformities of scaphoid nonunion are time dependent and predictable.[10] Such changes,

From the Department of Orthopaedic Surgery, Osaka University Graduate School of Medicine, Suita, Osaka, Japan.

Received for publication May 9, 2005; accepted in revised form August 11, 2005.

No benefits in any form have been received or will be received from a commercial party related directly or indirectly to the subject of this article.

Supported by the New Energy and Industrial Technology Development Organization of Japan (T.M.).

Corresponding author: Kunihiro Oka, MD, Department of Orthopaedic Surgery, Osaka University Graduate School of Medicine, 2-2, Yamadaoka, Suita, Osaka 565-0871, Japan; e-mail: oka-kunihiro@umin.ac.

0363-5023/05/30A06-0005$30.00/0
doi:10.1016/j.jhsa.2005.08.004

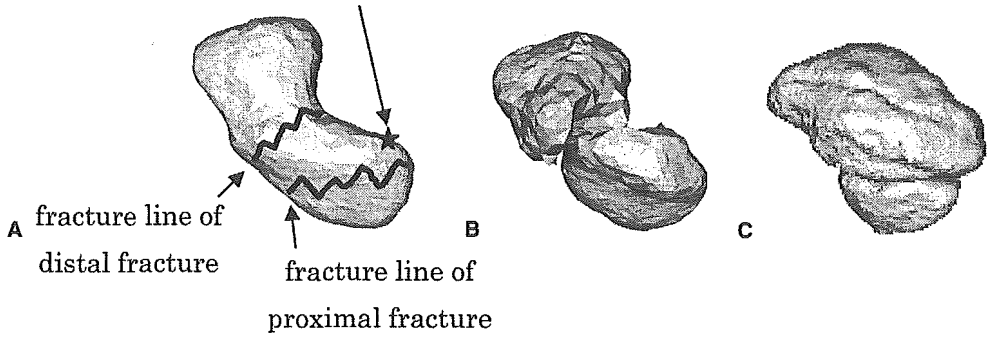

Figure 1. (A) Fracture location of a scaphoid nonunion based on the dorsal apex of the ridge from a dorsal view. (B) Distal fracture. (C) Proximal fracture.

however, do not occur in all cases of long-standing scaphoid nonunion.[11,12] Nakamura et al[13] classified deformity of scaphoid nonunion into 2 different types: (1) a volar type, in which the distal fragment overlaps the proximal fragment volarly, and (2) a dorsal type, in which the distal fragment overlaps the proximal fragment dorsally. Moritomo et al[14] suggested that the fracture level of scaphoid nonunion affects the pattern of deformity. They measured fracture location using the apex of the dorsal ridge of the scaphoid (where the dorsal intercarpal ligament and the dorsal part of the dorsal scapholunate interosseous ligament [DSLIL] are attached) as an anatomic landmark. They reported that in volar-type nonunion all cases exhibited DISI deformity and the fracture line generally was distal to the apex of the dorsal ridge of the scaphoid, and that in dorsal-type nonunion none of the cases showed DISI deformity and the fracture line was proximal to the apex of the dorsal ridge of the scaphoid. Our study involved quantification of the displacement of scaphoid nonunion and characterization of the displacement of the lunate, triquetrum, and capitate. Our purpose was to quantify the deformity of the carpus in scaphoid nonunion based on the fracture line and to clarify the mechanism of development of the associated degenerative change.

Materials and Methods

The study comprised 20 patients (17 men, 3 women) with established scaphoid nonunions. The mean patient age was 33.7 years (range, 18–75 y) and the mean interval between injury and examination was 89.9 months (range, 3.0–480 mo). Thirteen patients had not sought any treatment for the original fracture, 6 patients who were misdiagnosed as having a simple sprain received no immobilization, and 1 patient had been immobilized in a cast. By using 3-dimensional modeling the 20 scaphoid nonunions were divided into 2 groups according to the classification of Moritomo et al.[14] Nonunions were classified as distal fracture (n = 16) if the fracture line was distal to the dorsal apex of the scaphoid ridge and as proximal fracture (n = 4) if the line was proximal to this landmark (Fig. 1). The median interval from injury to examination was 16.2 months (range, 3.0–480.0 mo) for distal fractures and 64.4 months (range, 8.6–97.0 mo) for proximal fractures. The cases of scaphoid fractures for which intervals were less than 6 months were considered to be nonunions when they were accompanied with sclerotic margins, an enlarging cyst, or progressive collapse.

Image Acquisition

We performed computed x-ray tomography on both wrists using a slice thickness of 0.625 mm obtained on a clinical helical type scanner (LightSpeed Ultra 16; General Electric, Maukesha, WI). With the patient prone and the arms elevated and extended overhead we maintained a neutral position with an orthosis. Data were saved in a standard format (Digital Imaging and Communications in Medicine [DICOM]) that is used commonly for transferring and storing medical images.

Segmentation and Construction of a 3-Dimensional Surface Bone Model

Segmentation is defined as extracting bone regions and associating each region with individual bones. The anatomic structure or region of interest must be delineated and separated so that it can be viewed individually and 3-dimensional bone models can be reconstructed. Regions of individual bones were segmented semiautomatically by using software (Virtual Place-M; AZE, Ltd., Tokyo, Japan). Surface models of each carpal bone, the radius, and the ulna were

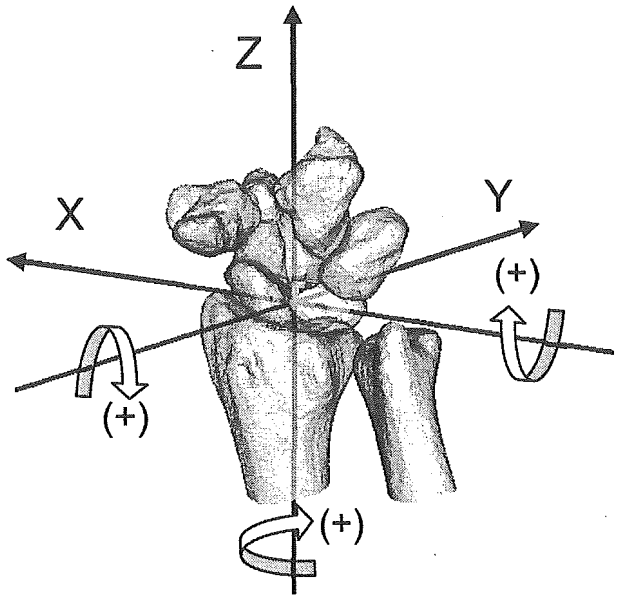

Figure 2. Orthogonal reference axis system. The *x*-axis is the line running from the radial styloid process to ulnar, the *y*-axis is the axis of the radius, and the *z*-axis is the line normal to the *xy* plane. Clockwise rotation is positive.

obtained by performing 3-dimensional surface generation of the bone cortex.[15]

Registration

To measure the deformity of the carpus we used the orthogonal reference system of Belsole et al[16] and we calculated the displacement by matching the injured hand with the mirror image of the contralateral uninjured hand. The carpus and radius were registered with the mirror images of the contralateral uninjured hand using an independent implementation of the iterative closest-point registration algorithm.[17] For scaphoid nonunion the distal and proximal fragment models were matched separately.

Quantification of Displacement

The injured hand was compared with the mirror image of the contralateral uninjured hand by superimposing one on the other. Also the displacements of the distal fragment, proximal fragment, lunate, triquetrum, and capitate were visualized and quantified. In this analysis of displacement an orthogonal reference axis system (Fig. 2) was established for the right wrist. Scaphoid nonunion of the left hand was converted to the right hand. The *x*-axis was defined as a line running through 2 points—the styloid processes of the radius and ulna—and indicated the radial(+)/ulnar(–) direction. The *z*-axis was defined as the longitudinal radial axis and indicated the distal(+)/proximal(–) direction. The *y*-axis was defined as the line normal to the *xz* plane and indicated the volar(+)/dorsal(–) direction. Clockwise rotation was defined as a positive angle. Rotation around the *x*-axis produced flexion(+) and extension(–), rotation around the *y*-axis produced ulnar(+) and radial(–) deviation, and rotation around the *z*-axis produced supination(+) and pronation(–). The rotation angles of displacement were calculated first about the *x*-axis (ulnoradial), next about the *y*-axis (proximodistal), and last about the *z*-axis (dorsopalmar). The rotational displacements of the distal fragment, proximal

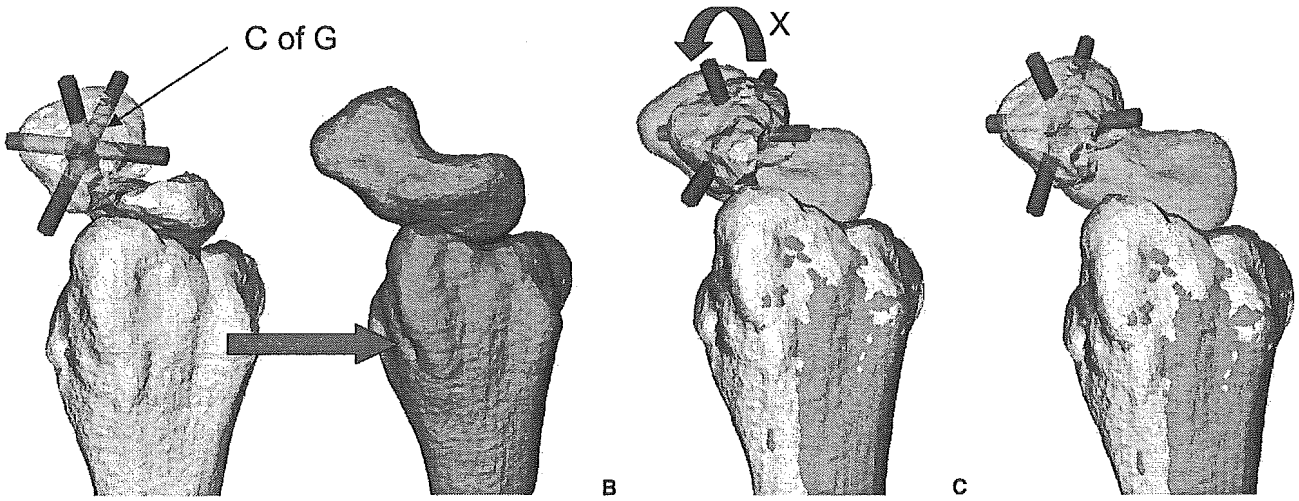

Figure 3. The center of mass of the distal fragment can be computed from its volume data of the surface model. (A) The radius of the affected side with the distal scaphoid fragment was superimposed on the mirror image of the contralateral radius. The distal scaphoid fragment (B) was superimposed on the distal part of the mirror image of the contralateral normal scaphoid (C). The translation of the center of mass of the distal scaphoid fragment (X) can be measured.

Table 1. Displacement of the Proximal Row

			Proximal Fragment of the Scaphoid (deg)			Distal Fragment of the Scaphoid (deg)			Lunate (deg)			Triquetrum (deg)		
Type	Case	Duration (mo)	*x*	*y*	*z*	*x*	*y*	*z*	*x*	*y*	*z*	*x*	*y*	*z*
Proximal	1	8.6	−3.8	−2.1	−0.3	−0.2	−1.6	−1.6	−4.3	−5.6	1.3	−15.2	−3.8	1.6
Proximal	2	36.0	1.7	−7.2	−10.2	1.6	2.1	−5.2	−3.7	−3.4	−2.9	−5.6	1.1	2.6
Proximal	3	92.7	−3.3	4.2	4.4	8.5	4.8	−5.9	0.1	4.6	3.6	−0.3	−0.5	−2.6
Proximal	4	97.0	−27.4	10.0	−6.6	0.2	14.2	−4.0	−13.8	6.4	−0.2	−5.8	5.3	3.4
Average		(Median: 64.4)	−8.2	1.2	−3.2	2.5	4.9	−4.2	−5.4	0.5	0.5	−6.7	0.5	1.3
Distal	5	3.0	−28.9	−5.9	9.4	−8.4	−1.4	−9.1	−11.5	−3.8	1.9	−7.4	−4.6	3.8
Distal	6	3.0	−47.9	10.7	22.2	−12.4	10.1	−21.5	−18.6	6.8	3.2	−14.0	0.3	5.1
Distal	7	3.1	−24.5	4.0	11.2	−8.7	−4.0	−4.7	−13.7	−8.9	−3.3	−13.1	−6.2	−1.8
Distal	8	5.6	−25.1	1.4	5.5	2.5	5.0	0.1	−16.5	0.5	3.0	−10.1	−1.4	−4.1
Distal	9	5.9	−33.0	15.7	16.1	−6.0	4.0	−8.4	−8.5	4.4	−2.6	−4.8	1.4	−0.1
Distal	10	7.1	−46.0	8.3	37.8	7.5	16.9	−18.8	−29.9	7.8	12.9	−19.8	11.8	7.4
Distal	11	8.9	−25.1	−1.3	9.5	3.1	4.1	1.9	−12.6	2.2	4.8	−7.9	−0.1	5.1
Distal	12	13.4	−48.7	−7.9	25.9	12.2	11.2	−17.7	−26.9	−0.3	12.9	−18.7	−2.5	10.6
Distal	13	19.0	−16.8	8.6	3.1	−12.5	8.0	1.3	−13.3	10.2	3.0	−12.5	8.0	1.3
Distal	14	61.9	−27.0	−1.1	26.4	12.0	13.7	−17.3	−12.2	−0.1	9.1	−7.7	−6.5	−4.0
Distal	15	111.0	−48.6	−4.6	33.1	−1.5	8.3	−4.3	−27.8	−1.4	13.7	−19.5	1.3	7.7
Distal	16	161.0	−32.2	4.6	18.8	−23.0	3.0	7.0	−15.3	1.0	7.6	−12.6	−1.8	−2.6
Distal	17	192.0	−28.9	−2.0	25.2	44.1	38.4	−44.0	−10.8	−1.2	14.3	−4.9	−0.5	13.7
Distal	18	240.0	−29.2	7.2	13.9	−11.1	−7.9	10.0	−13.3	6.7	4.2	−7.0	−2.3	3.6
Distal	19	250.0	−62.5	6.6	28.7	7.2	6.4	15.3	−27.7	0.4	1.8	−23.5	4.6	1.5
Distal	20	480.0	−45.8	−10.0	19.8	−11.3	6.7	−4.0	−22.0	−12.2	1.5	−12.2	−8.2	0.9
Average		(Median: 16.2)	−35.6	2.1	19.2	−0.4	7.7	−7.1	−17.5	0.8	5.5	−12.2	−0.4	3.0

NOTE. Rotation around the *x*-axis produces flexion(+) and extension(−), rotation around *y*-axis produces ulnar(+) and radial(−) deviation, and rotation around *z*-axis produces supination(+) and pronation(−).

fragment, lunate, and triquetrum were calculated around these orthogonal reference axes. We defined DISI deformity as a situation in which lunate extension around the *x*-axis increased by more than 10° compared with the contralateral side.For the capitate and the distal fragment of the scaphoid we computed the center of mass[18] using the volume data of the surface model of each component and calculated the translation of these points (Fig. 3), which indicated the 3-dimensional vector relative to an orthogonal reference axis (Fig. 2).

Results

Results are listed in Tables 1 and 2.

Distal Fractures

The deformities of the proximal row in scaphoid nonunion with distal fractures (n = 16) are shown in Figure 4A. The surface models of the affected side (dark-colored parts) were superimposed on the mirror image of the contralateral uninjured side (gray-colored parts) relative to the radius. The proximal fragment of the scaphoid, lunate, and triquetrum (dark-colored parts) rotated into extension and supination relative to the normal proximal row (gray-colored parts). For the proximal fragment of the scaphoid the mean extension was 35.6° ± 12.5° and the mean supination was 19.2° ± 10.0°. For the lunate the mean extension was 17.5° ± 7.0° and the mean supination was 5.5° ± 5.6°. For the triquetrum the mean extension was 12.2° ± 5.7° and the mean supination was 3.0° ± 5.1°. Dorsal intercalated segment instability deformity was observed in 15 of the 16 cases with distal fractures. The distal fragment of the scaphoid and the capitate showed small angles of rotation but they translated together dorsally 3.13 ± 1.46 mm and 2.46 ± 1.17 mm, respectively (Fig. 4B). Only the distal scaphoid fragment and the capitate of the affected side (dark-colored parts) are shown in Figure 4B to show more easily the dorsal translation relative to the normal position (gray-colored parts).

Proximal Fractures

The deformity was less marked for proximal fractures (n = 4) than for distal fractures (Fig. 5). For the proximal fragment of the scaphoid the mean extension was 8.2° ± 13.0° and the mean prona-